

The Polymerization of Homogentisic Acid In Vitro as a Model for Pyomelanin Formation

Hanaa A. Galeb, Angelo Lamantia, Alexander Robson, Katja König, Jonas Eichhorn, Sara J. Baldock, Mark D. Ashton, John V. Baum, Richard L. Mort, Benjamin J. Robinson,* Felix H. Schacher,* Victor Chechik,* Adam M. Taylor,* and John G. Hardy*

Melanins are a class of biopolymers that are widespread in nature, with diverse origins, compositions, and functions, and their chemical and optoelectronic properties render them potentially useful for application in materials science for various biotechnological applications. For patients with alkaptonuria, the accumulation of homogentisic acid (HGA) in their bodies is associated with the concomitant deposition of pyomelanin, which is a pigment that contains significant amounts of polymerized HGA (polyHGA) in the bodily tissues of the patients. The polymerization of HGA under various different conditions in vitro is investigated using a selection of different analytical chemistry techniques to understand if there may be a correlation between the conditions and pigment deposition in vivo, and their potential for application as green/sustainable and components of electronic devices.

red/yellow pheomelanins,^[2,3] all of which are present in the skin/hair.^[4] Melanins fulfill a variety of roles in nature (including photoprotection to photosensitization,^[4,5] antioxidant defense and metal/drug binding),^[6,7] which reflect their combination of chemical/electrical/optical/paramagnetic properties.^[8,9] Such properties facilitate their application in materials science for a range of medical and technical applications.^[9,10]

Melanin production is typically an oxidative process involving reactive oxygen species occurring in vivo, often also involving enzymes such as oxidases (e.g., phenolases that catalyze the oxidation of phenol derivatives (eumelanins and pheomelanins


are produced within melanocytes by a complex biosynthetic pathway)) followed by uncontrolled polymerization of the oxidized intermediates (often involving a reactive quinone intermediate prone to reactions with amine and hydroxyl groups and capable of undergoing reversible redox reactions).^[3] In contrast to the

1. Introduction

Melanins are a class of biopolymers with diverse origins, compositions, and colors, from black/brown eumelanins^[1] to

H. A. Galeb, A. Robson, S. J. Baldock, M. D. Ashton, J. V. Baum, J. G. Hardy
Department of Chemistry
Lancaster University
Lancaster LA1 4YB, UK
E-mail: j.g.hardy@lancaster.ac.uk
H. A. Galeb
Department of Chemistry, Science and Arts College, Rabigh Campus
King Abdulaziz University
Jeddah 21577, Saudi Arabia
A. Lamantia, B. J. Robinson
Department of Physics
Lancaster University
Lancaster LA1 4YW, UK
E-mail: b.j.robinson@lancaster.ac.uk

K. König, J. Eichhorn, F. H. Schacher
Institut für Organische und Makromolekulare Chemie
Friedrich-Schiller-Universität Jena
Lessingstraße 8, Jena 07743, Germany
E-mail: felix.schacher@uni-jena.de
R. L. Mort
Division of Biomedical and Life Sciences
Lancaster University
Lancaster LA1 4YG, UK
B. J. Robinson, J. G. Hardy
Materials Science Institute
Lancaster University
Lancaster LA1 4YB, UK
V. Chechik
Department of Chemistry
University of York
Heslington, York YO10 5DD, UK
E-mail: victor.chechik@york.ac.uk
A. M. Taylor
Lancaster Medical School
Lancaster University
Lancaster LA1 4YW, UK
E-mail: a.m.taylor@lancaster.ac.uk

 The ORCID identification number(s) for the author(s) of this article can be found under <https://doi.org/10.1002/macp.202100489>

© 2022 The Authors. Macromolecular Chemistry and Physics published by Wiley-VCH GmbH. This is an open access article under the terms of the Creative Commons Attribution License, which permits use, distribution and reproduction in any medium, provided the original work is properly cited.

DOI: 10.1002/macp.202100489

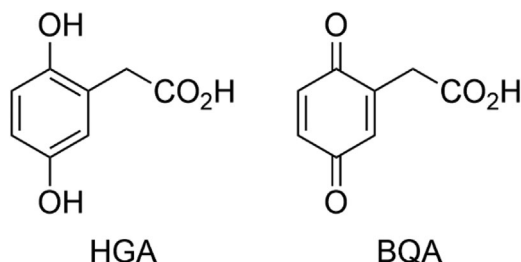


Figure 1. The chemical structures of homogentisic acid (HGA) and benzoquinone acetic acid (BQA).

production of polynucleic acids (e.g., DNA and RNA) and proteins, melanin production does not involve “templates” and, therefore, the compositions, connectivity, and sequences of “monomers” in the backbone of the melanins are random (albeit clearly influenced by the feedstocks available, organism/tissue, and other conditions). Various melanins exist, each of which is rich in certain monomers: eumelanins (L-dopa),^[11] pheomelanin (5-cys-dopa),^[11] neuromelanins (5,6-dihydroxyindole),^[12,13] catechol melanins (catecholic monomers),^[14,15] insect melanin (*N*-acetyl-dopamine),^[16,17] alloxanins (1,8-dihydroxynaphthalene),^[3,18] and pyomelanin (homogentisic acid (HGA) and potentially a benzoquinone derivative (benzoquinone acetic acid, BQA^[19]); **Figure 1**).^[20] The polymerization of melanins^[21] yields species with high molecular weights and often the formation of insoluble pigment^[22] (the formation of which is proposed to proceed via a nucleation and growth mechanism),^[23] and the structures, properties, and applications of natural and synthetic melanins have been reviewed.^[11,21,24–30]

Pyomelanins and ochronotic pigment formation can be driven enzymatically or indeed via autopolymerization in the presence of oxygen in a variety of prokaryotic/eukaryotic species. Eukaryotic organisms contain a variety of enzymes in varying concentrations in different intracellular/extracellular environments, and therefore studies to understand the polymerization of HGA in various conditions may offer insight into the deposition of pyomelanin pigmentation in various tissues (of importance for diseases like alkaptonuria).

Here we report the results of an investigation of the polymerization of HGA to form polyHGA (a simplified version of pyomelanin, **Figure 2**) in the absence or presence of enzymes (a laccase (LACC),^[31] peroxidase (horseradish peroxidase (HRP)), or tyrosinase (TYR)) at either pH 5.0 or 7.4. A selection of different analytical techniques was applied to study the resultant pyomelanins, including UV-vis spectroscopy, nuclear magnetic resonance (NMR) spectroscopy, X-ray photoelectron spectroscopy (XPS), size exclusion chromatography (SEC), dynamic light scattering (DLS), scanning electron microscopy (SEM), energy-dispersive X-ray (EDX) spectroscopy, Fourier-transform infrared (FTIR) spectroscopy, electron paramagnetic resonance (EPR) spectroscopy, cyclic voltammetry (CV), and conductive probe atomic force microscopy (C-AFM). Condition-dependent polyHGA formation was observed, which offers insight into real-world observations of pyomelanin pigment deposition inside specific tissues in the body (e.g., observed by eye or histological studies),^[32–35] and moreover, highlights their potential for optimization for utilization in electronic devices.^[27]

2. Results and Discussion

The product of the polymerization of HGA (**Figure 1**) was studied in the absence (control) or presence of enzymes (a laccase,^[31,36] peroxidase, or tyrosinase) at either pH 5 or 7.4 with a view to understand the potential role of enzymes and pH on the formation of ochronotic pigment (**Figure 2**).

There were discernible differences in the color of the reaction mixtures within hours (with solutions at pH 5 somewhat lighter in color than those at pH 7.4), and the reaction mixtures proceeded to become significantly darker over the period of weeks, which is the characteristic of pyomelanins (**Figure S1**, Supporting Information). The addition of tyrosinase to HGA when compared to the control experiment in the absence of tyrosinase showed discernible differences in the UV-vis spectra (**Figure S2**, Supporting Information), with the appearance of a second peak at 250 nm due to the oxidation of HGA to BQA (in addition to the characteristic peak of HGA at 290 nm),^[37] which was more pronounced for experiments carried out at pH 7.4 than at pH 5. UV-vis spectra were recorded over 24 h using a concentration of HGA of 10.4 mg mL⁻¹ to avoid complications with precipitate formation and light

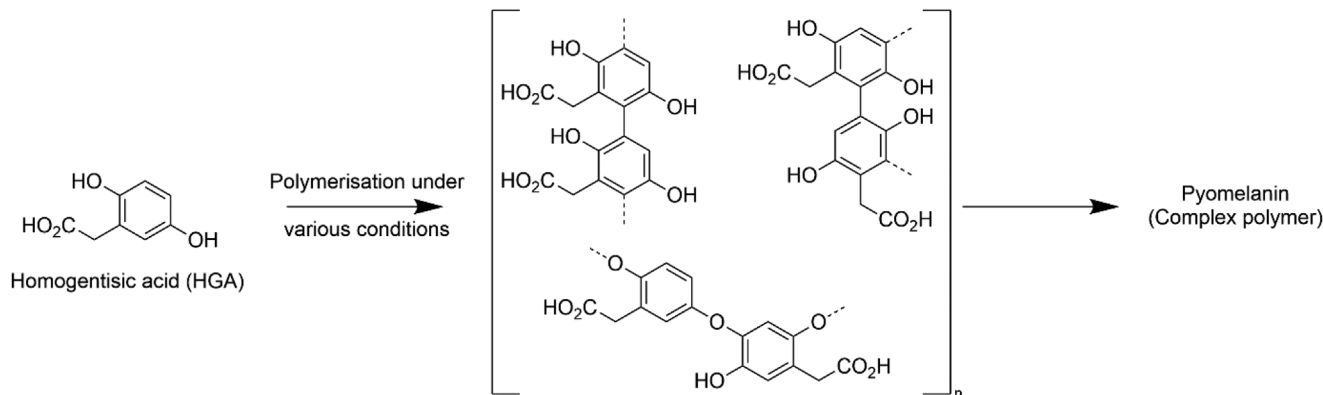


Figure 2. A schematic of the polymerization of homogentisic acid (HGA) to form pyomelanin. It is important to note that pyomelanin may contain other monomers depending on the conditions under which they are formed in vivo, and a simplified version of pyomelanin, polyHGA (depicted above), is studied herein.

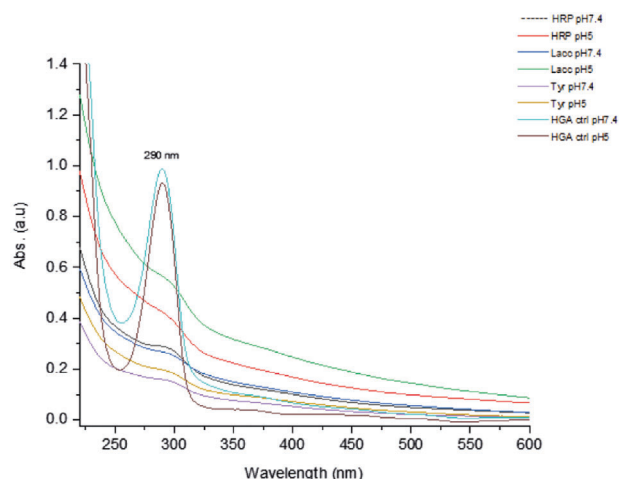


Figure 3. UV-vis spectra of HGA reaction mixtures after 6 weeks at either pH 5.0 or 7.4, in the absence of enzyme (control) or presence of enzyme (laccase (LACC), peroxidase (HRP), tyrosinase (TYR)).

scattering/precipitation complicating UV-vis spectra recording and/or interpretation over the period of the experiment. UV-vis spectra showed that using a laccase or peroxidase produced significantly more polyHGA than tyrosinase or the no-enzyme control, with polyHGA production being condition dependent, with peroxidase \geq laccase $>$ tyrosinase \approx no enzyme control (Figure S2, Supporting Information). It is important to note that each enzyme works best at a specific optimal pH value, and deviations in pH from the optimal may result in a decrease in activity due to alterations in the shape of the enzyme's active site, and the subtle differences in the pH dependence of the UV-vis spectra are in line with literature (laccases,^[38] peroxidases,^[39,40] tyrosinases,^[41]

and HGA autopolymerization at high pH values^[32,37] (albeit outside the physiologically relevant pH range for humans)^[42] and are also suggestive of various oxidation states of the monomeric units constituting the backbone of the polyHGAs.

The corresponding percentage yields of the polyHGA precipitate isolated by lyophilization after 5 days of reaction using a concentration of HGA of 10.4 mg mL^{-1} , followed by dialysis (molecular weight cutoff of 3.5 kDa) showed a similar trend: peroxidase \geq laccase $>$ tyrosinase \approx no enzyme control (percentage yields of $\approx 11 \pm 2\%$, $\approx 11 \pm 8\%$, $\approx 7 \pm 2\%$, and $\approx 6 \pm 2\%$, respectively, at pH 5; $\approx 21 \pm 4\%$, $\approx 7 \pm 3\%$, $\approx 5 \pm 1\%$, and $\approx 5 \pm 2\%$, respectively, at pH 7.4). To produce sufficient melanin for analysis via other techniques, experiments were carried out under analogous conditions with the concentration of HGA of 33.6 mg mL^{-1} for longer periods of time (6 weeks) yielding polyHGA showing a broadband absorption typical of melanins (Figure 3; Figure S1, Supporting Information).

While the ^1H NMR spectra recorded in D_2O of HGA show characteristically sharp peaks for the three aromatic protons and two alkyl protons ($\text{Ar}-\text{CH}_2-\text{CO}_2\text{H}$) on HGA (Figure S3, Supporting Information), after polymerization for 6 weeks the ^1H NMR spectrum for the polyHGA (no enzyme control at pH 5) is sharp indicative of relatively little polymerization in line with the mass isolated (Figures S4, Supporting Information), whereas the ^1H NMR spectra for the other polyHGAs typically have broad lines suggesting the polymers have high molecular weights and/or aggregation of the oligomers/polymers, which is the characteristic of melanins (Figures S5–S11, Supporting Information). In principle, it may be possible to estimate the ratio of $\text{Ar}-\text{Ar}/\text{C}-\text{C}$ bonds to $\text{Ar}-\text{O}-\text{Ar}/\text{C}-\text{O}-\text{C}$ bonds from the ratio of aromatic:alkyl protons (Table 1), with a ratio of 2:3 alkyl:aromatic protons indicative of no/minimal reaction (e.g., HGA control and no enzyme control at pH 5) or formation of $\text{Ar}-\text{O}-\text{Ar}/\text{C}-\text{O}-\text{C}$ bonds, and

Table 1. Summary of data of polyHGAs from various reaction conditions.

Functionality	^1H NMR Integral of alkyl (C–H)	^1H NMR Integral of aromatic (C–H)	^1H NMR Spectrum	XPS (Table summary of C 1s and O 1s data)	SEM-EDX	I–V curves
HGA	2	3.00	Figure S3 (Supporting Information)	Table S1 (Supporting Information)	N/A.	N/A.
PolyHGA (no enzyme control at pH 5.0)	2	3.00	Figure S4 (Supporting Information)	Table S2 (Supporting Information)	Figure S16 (Supporting Information)	N/A.
PolyHGA (no enzyme control at pH 7.4)	2	2.32	Figure S5 (Supporting Information)	Table S2 (Supporting Information)	Figure S17 (Supporting Information)	N/A.
PolyHGA (tyrosinase at pH 5.0)	2	0.99	Figure S6 (Supporting Information)	Table S3 (Supporting Information)	Figure S18 (Supporting Information)	Figure S31 (Supporting Information)
PolyHGA (tyrosinase at pH 7.4)	2	0.89	Figure S7 (Supporting Information)	Table S3 (Supporting Information)	Figure S19 (Supporting Information)	Figure S32 (Supporting Information)
PolyHGA (laccase at pH 5.0)	2	1.62	Figure S8 (Supporting Information)	Table S4 (Supporting Information)	Figure S20 (Supporting Information)	Figure S33 (Supporting Information)
PolyHGA (laccase at pH 7.4)	2	0.91	Figure S9 (Supporting Information)	Table S4 (Supporting Information)	Figure S21 (Supporting Information)	Figure S34 (Supporting Information)
PolyHGA (peroxidase at pH 5.0)	2	1.79	Figure S10 (Supporting Information)	Table S5 (Supporting Information)	Figure S22 (Supporting Information)	Figure S35 (Supporting Information)
PolyHGA (peroxidase at pH 7.4)	2	1.55	Figure S11 (Supporting Information)	Table S5 (Supporting Information)	Figure S23 (Supporting Information)	Figure S36 (Supporting Information)

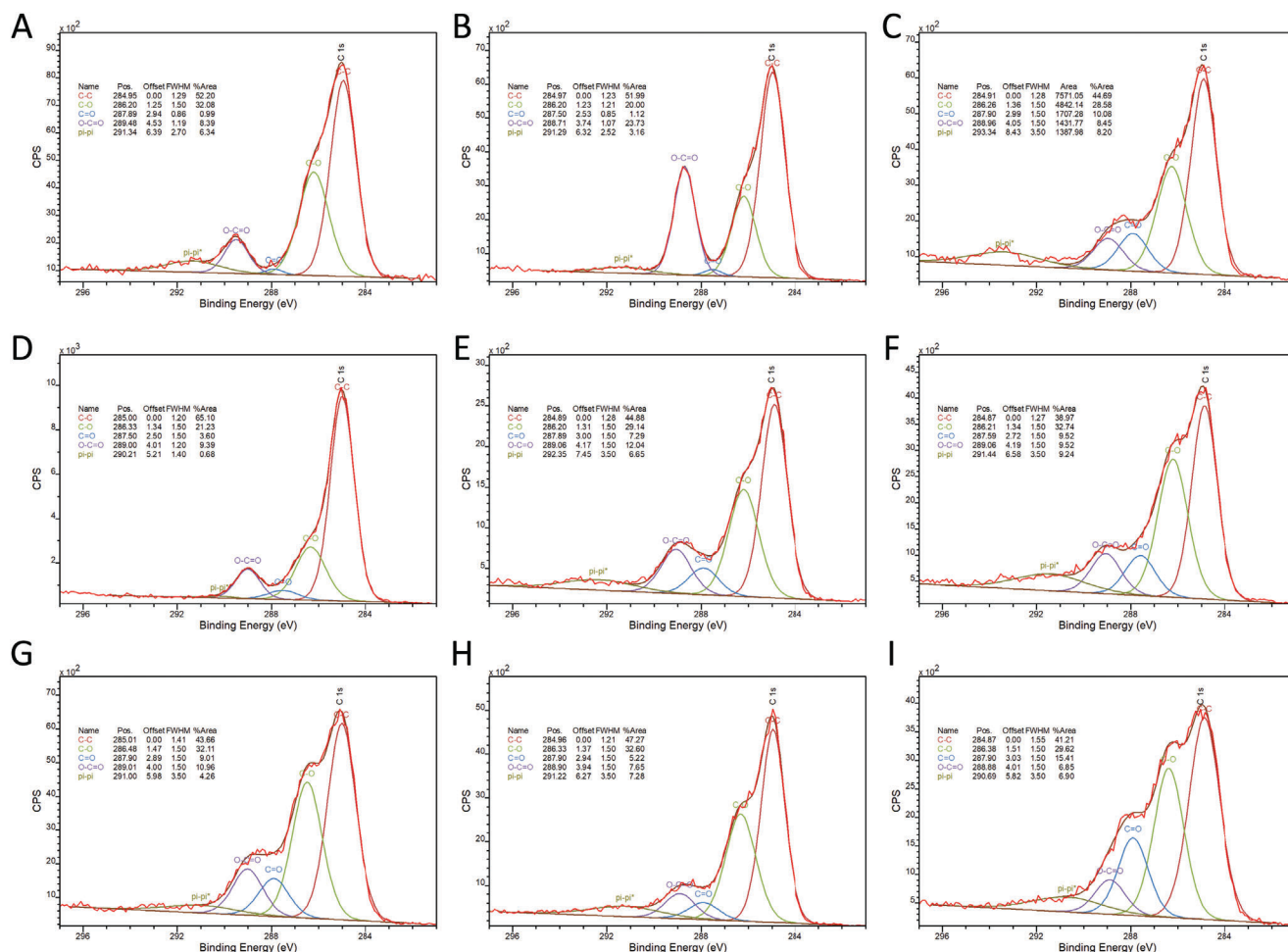


Figure 4. XPS C 1s core line spectra: A) HGA; B) polyHGA (no enzyme control at pH 5.0); C) polyHGA (no enzyme control at pH 7.4); D) polyHGA (formed in the presence of tyrosinase at pH 5.0); E) polyHGA (formed in the presence of tyrosinase at pH 7.4); F) polyHGA (formed in the presence of laccase at pH 5.0); G) polyHGA (formed in the presence of laccase at pH 7.4); H) polyHGA (formed in the presence of peroxidase at pH 5.0); and I) polyHGA (formed in the presence of peroxidase at pH 7.4).

deviation from that ratio indicative of formation of a greater proportion of Ar–Ar/C–C bonds, which is suggested by our data. It is noteworthy that our data are in line with solid-state NMR studies of monomer connectivity in pyromelanins,^[36] and studies of pH dependence of polymerization of phenolic compounds suggest the preference for C–C bond formation instead of C–O–C bond formation at the pH values employed in this study with various enzymes (cognizant of the fact that enzymes function best at a specific optimal pH value at which the shape of the enzyme's active site is optimal for function with specific substrates);^[43–47] furthermore, polymers connected via C–O–C bonds are expected to have lower electrical conductivity than polymers connected via C–C bonds akin to graphene derivatives.^[48]

XPS data (Figures 4 and 5; Figures S12–S14 and Tables S1–S5, Supporting Information) confirmed that the HGA and polyHGAs were predominantly composed of C and O (with traces of N (residual enzyme), Na/Cl (residual buffer), and Si (substrate)). The C 1s spectra confirmed the presence of C–C, C–O, C=O, O–C=O, and π – π bonds; and the O 1s spectra confirmed the presence of C=O and C–O bonds, and a Na KLL Auger peak,

which overlaps the O 1s envelope at ≈ 536 eV. There were no clear trends in the data to determine the connectivity of the polyHGA backbone^[49] (e.g., ratio of Ar–Ar/C–C bonds to Ar–O–Ar/C–O–C bonds normalized against the peak for O–C=O; Tables S1–S5, Supporting Information), and the varying levels of C=O bonds (plausibly due to both carboxylic acids and quinones) are suggestive of differing oxidation states for the monomers incorporated in the backbone of the polyHGAs.

SEC has previously been used to assess the molecular weight distributions of soluble oligomeric/polymeric melanin derivatives^[27,32] of the polyHGA after dialysis (molecular weight cutoff of 3.5 kDa) showed traces of the low-molecular-weight species and/or oligomeric species; however, higher-molecular-weight species (>3.5 kDa) were not observed due to removal of the aggregates on the guard column of the SEC (Figure S15, Supporting Information). DLS^[50] of the same samples showed no higher-molecular-weight species (>3.5 kDa) due to removal of the aggregates during filtration prior to DLS as part of standard sample preparation protocols. SEM was used in combination with EDX spectroscopy to assess the precipitate morphol-

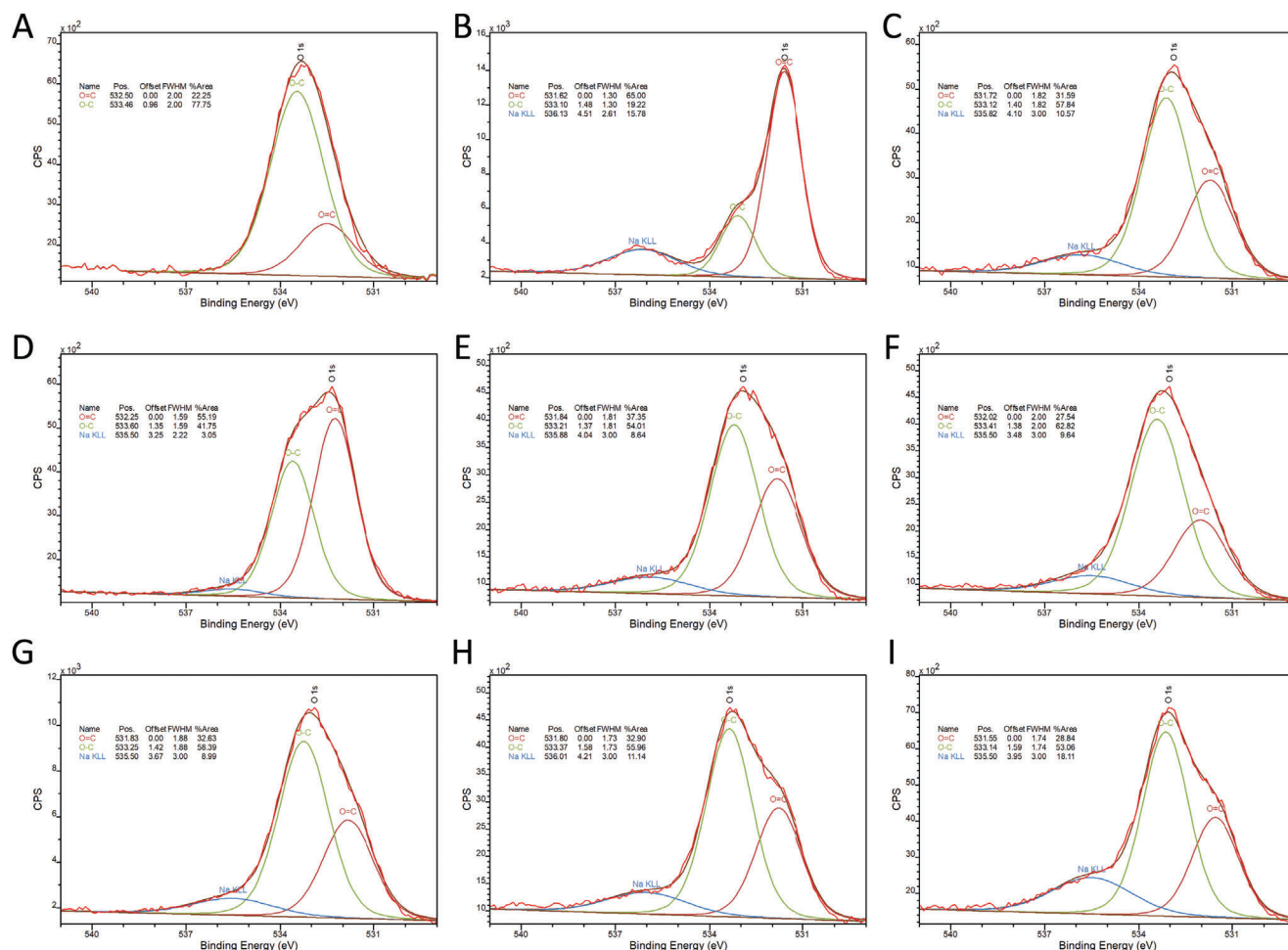


Figure 5. XPS O 1s core line spectra: A) HGA; B) polyHGA (no enzyme control at pH 5.0); C) polyHGA (no enzyme control at pH 7.4); D) polyHGA (formed in the presence of tyrosinase at pH 5.0); E) polyHGA (formed in the presence of tyrosinase at pH 7.4); F) polyHGA (formed in the presence of laccase at pH 5.0); G) polyHGA (formed in the presence of laccase at pH 7.4); H) polyHGA (formed in the presence of peroxidase at pH 5.0); and I) polyHGA (formed in the presence of peroxidase at pH 7.4).

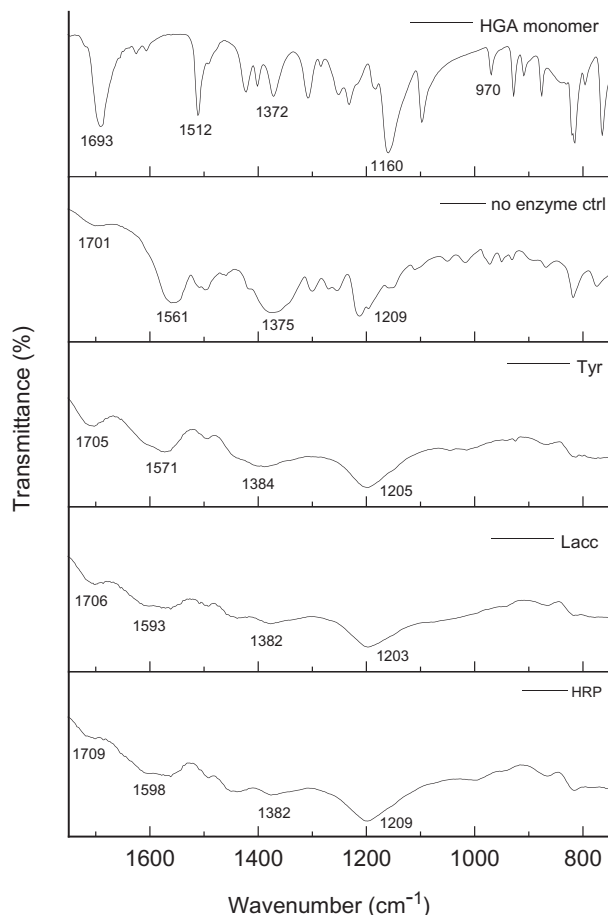
ogy and the elemental composition of the polyHGAs produced. SEM data show that the precipitates isolated were irregularly shaped with sizes between tens to hundreds of micrometers (Figures S16–S24, Supporting Information). There is no meaningful shape/size correlation as the polyHGAs are produced under unconstrained conditions, whereas the *in vivo* polyHGA precipitate shapes/sizes would be constrained by the intracellular/extracellular environment in which they are produced. EDX data suggest that all samples are mainly composed of C and O (similar to the XPS data) with additional K and Na from the buffer, Au (sputter coating), Si (substrate), and samples with enzymes also have traces of additional Al, Ca, Mg, and S (Figures S16–S23, Supporting Information).

FTIR spectroscopy was used to analyze the HGA and polyHGAs produced. The FTIR spectrum for the polyHGA (no enzyme control at pH 5) closest to the monomeric HGA is indicative of relatively little polymerization in line with the mass isolated; however, all other polyHGAs had significantly broader peaks than monomeric HGA, as expected for polymeric species with a variety of chemical environments (Figure 6; Figure S25, Support-

ing Information). A discernible difference in the FTIR spectra of HGA and the polyHGAs was the broadening/diminution of the peak at $\approx 970\text{ cm}^{-1}$ in HGA (from the aromatic hydrogens) suggestive of C–C bond formation, with broadening of bands at $1500\text{--}1510\text{ cm}^{-1}$ (aromatic C=C bonds) and the weak band at $\approx 1580\text{ cm}^{-1}$ (aromatic C=C). Peaks at $\approx 1200\text{--}1210\text{ cm}^{-1}$ corresponding to phenolic OH and at $\approx 1560\text{--}1570\text{ cm}^{-1}$ corresponding to the C=O bond of the carboxylic acid functional groups are present in all spectra, albeit broader.^[31]

EPR spectroscopy was used to study the powders. X-band EPR spectra of all polyHGA powders showed nearly identical spectra (Figure 7). The spectra had a single peak centered at $g = 2.0035$, with a peak-to-peak width of $\approx 4\text{ G}$ (the polyHGA generated in the presence of tyrosinase at pH 5.0 gave a slightly broader peak with a peak-to-peak width of $\approx 4.6\text{ G}$). The polyHGA generated in the presence of peroxidase and no enzyme controls gave much more intense peaks than polyHGA generated in the presence of laccase or tyrosinase. This may be related to the extended conjugation length of the different polymers.^[51] In general, the EPR peak shape and width were similar to those of eume-

pH 5.0



pH 7.4

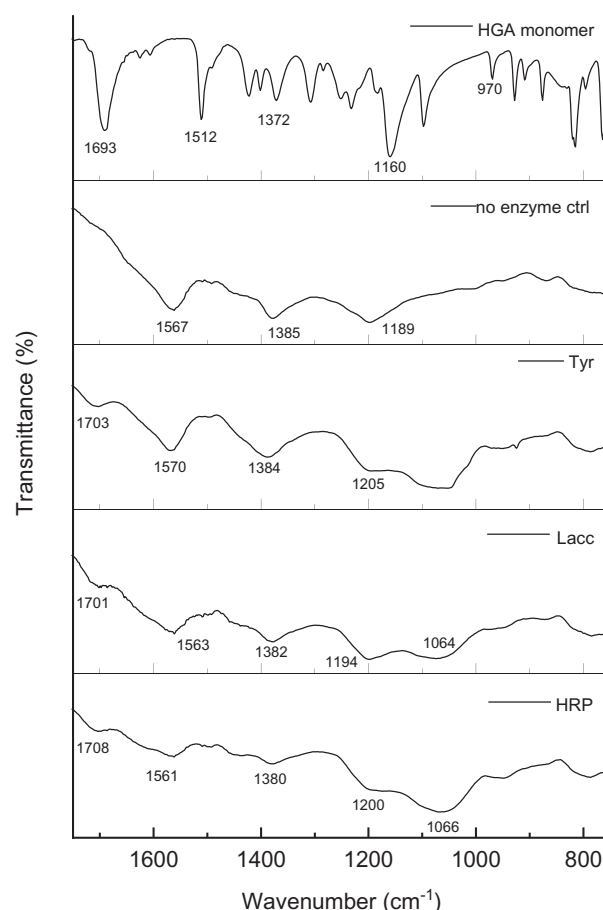


Figure 6. FTIR spectra of dialyzed polyHGA isolated after 6 weeks of reaction at pH 5.0 and pH 7.4, generated in the absence of enzyme (no enzyme control) or presence of enzyme (laccase (LACC), peroxidase (HRP), and tyrosinase (TYR)).

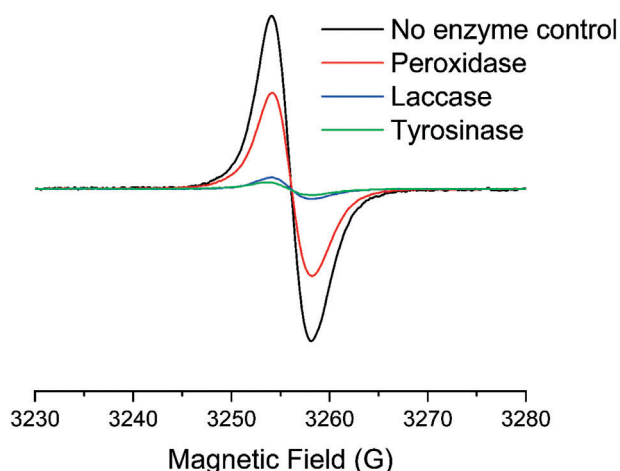


Figure 7. X-band EPR spectra of polyHGA samples generated at pH 7.4 in the absence of enzymes (black), or presence of laccase (blue), peroxidase (red), or tyrosinase (green).

lanins and consistent with the pyomelanin spectra reported in the literature.^[52]

A close inspection of the EPR peak of polyHGA showed a noticeable asymmetry. Spectrum simulation required two components to accurately reproduce the line shape (**Figure 8**; Figures S26–S28, Supporting Information). These components can be assigned to carbon-centered and semiquinone radicals based on their *g*-values (≈ 2.0034 and 2.0040 , respectively). All polyHGA spectra were dominated by the C-centered radical with ≈ 2 – 6% contribution of the semiquinone. This is similar to the precedent for eumelanins, although the contribution of the semiquinone radical in eumelanins is higher.^[53]

Recording EPR spectra under saturating conditions (at a high microwave power of up to 200 mW) did not reveal any fast-relaxing organic radical components. In some pyomelanin samples, a clear semiquinone signal was reported in the literature.^[31] The absence of this signal in our samples can be explained by the small contribution of the semiquinone radical to the overall EPR signal. The spectra recorded at high power, however, suggested the presence of some EPR-active metals in all enzyme-derived

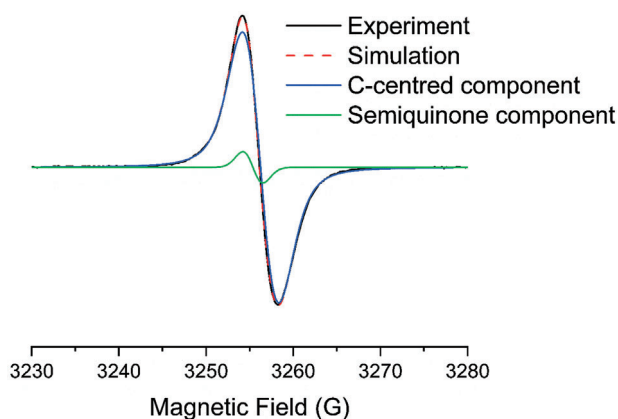


Figure 8. Experimental EPR spectrum of polyHGA generated in the presence of peroxidase sample (black) and simulation (red). The simulation included a broad C-centered component ($g = 2.0034$, Voigtian line shape with peak-to-peak width 4.2 G, 97.8%) and a sharper semiquinone radical ($g = 2.004$, Gaussian line shape with peak-to-peak width 2.2 G, 2.2%).

samples, possibly originating from the traces of residual enzymes (supported by EDX data; see Figures S16–S23 in the Supporting Information).

Cyclic voltammetry has previously been used to study the reduction/oxidation processes and electron-transfer properties of polyphenols analogous to polyHGA. Cyclic voltammetry of HGA shows a clear anodic peak due to the oxidation of HGA to BQA, and a clear cathodic peak due to the reduction of BQA to HGA, the positions of which are solvent and pH dependent.^[54,55] The cyclic voltammograms of the polyHGAs generated in this study at pH 5 (Figure S29, Supporting Information) show an anodic peak at ≈ 0.56 V and the corresponding cathodic peak at ≈ 0 V versus Ag/AgCl (reference electrode), whereas at pH 7.4 (Figure S29, Supporting Information) the oxidation and reduction peaks were not resolved, i.e., the polyHGAs were electroactive in acidic medium while electro-inactive in neutral medium, confirming the role of protons in the electroactivity of the polyHGA (akin to polycatechol films).^[56] The cyclic voltammograms are consistent after multiple scans, demonstrating their stability under the experimental conditions for the duration of the experiment, and their unsymmetrical cathodic and anodic peaks are attributed to the difference in background current and kinetic limitations.^[56]

Conductive tip AFM studies of the powders isolated from polyHGA formation under various conditions showed some to be measurably conductive (the setup is depicted in Figure S30 in the Supporting Information). The polyHGAs generated by auto-oxidation of HGA at either pH 5 or at pH 7.4 (i.e., no enzyme control) were neither measurably conductive nor the polyHGAs generated in the presence of tyrosinase at either pH 5 or at pH 7.4, or laccase at pH 5. However, the polyHGAs generated in the presence of laccase at pH 7.4 or peroxidase at either pH 5 or pH 7.4 were measurably conductive (**Figure 9**), with average $\log_{10} G$ values of -11.52 ± 0.28 , -8.52 ± 0.24 , or -9.30 ± 0.32 S, respectively (I - V curves are in Figures S31–S36 in the Supporting Information), and a comparison of $\log G$ counter maps is shown in Figure S37 (Supporting Information); i.e., conductivity (G) of $2.9 \times 10^{-3} \pm 1.1 \times 10^{-3}$, 0.58 ± 0.2 , or 3.4 ± 1.2 nS, respectively. The differences in the electronic properties of the polymers^[51,57] are

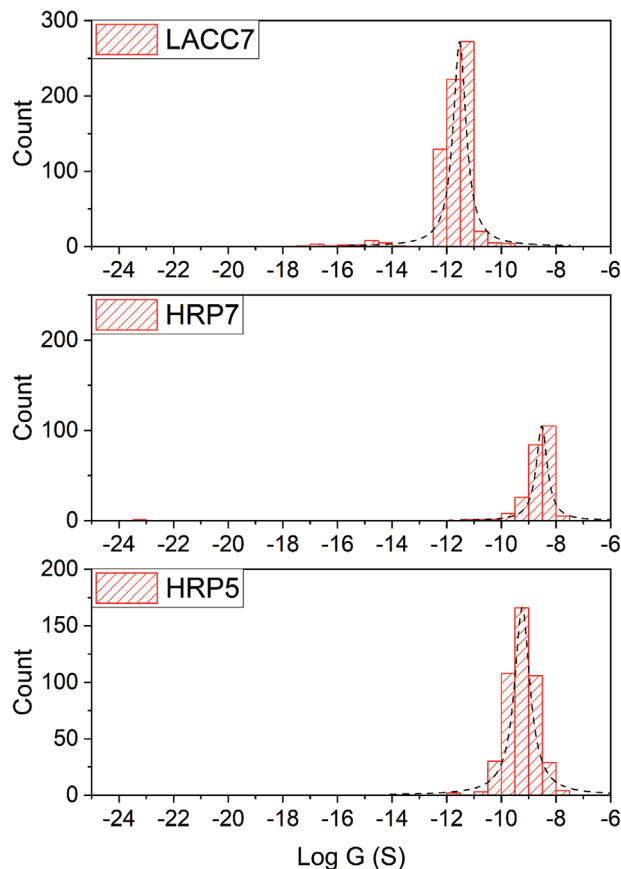


Figure 9. Conductive tip AFM data for polyHGAs. Comparison of the conductance histograms for polyHGAs generated in the presence of laccase (LACC) at pH 7.4, or peroxidase (HRP) at pH 7.4 or 5.0, respectively.

likely to be related to the extended conjugation length of the polyHGAs produced by laccase-/peroxidase-mediated polymerization of HGA, supported by the greater amounts of polyHGAs produced by laccase-/peroxidase-mediated polymerization of HGA and by EPR data (Figure 7). The polyHGAs produced have potential for application as green/sustainable^[58] and components of electronic devices,^[27,59–64] or other high value added applications (particularly after optimization of the synthesis).^[8,58,65–69]

The in vitro studies of the polymerization of HGA to form polyHGA (a simplified version of pyomelanin) described herein, investigated in the absence or presence of enzymes (a laccase, peroxidase, or tyrosinase) at physiologically relevant pH values (either pH 5.0 or 7.4), contribute to our understanding of real-world observations of pyomelanin pigment deposition inside specific tissues in the body (e.g., observed by eye or histological studies).^[32–35]

We note that enzyme activity is affected by various environmental factors (including, but not limited to, pH, salt concentration, and solvent), and the function of enzymes is governed by the primary sequence of the enzyme which is species specific, and systematic studies may offer insight into opportunities for industrial biotechnological approaches to melanin production.^[69–78] Recent advances in our analytical capabilities (e.g., single-cell analysis, and/or single-/multiomics (genomics, metabolomics,

proteomics, and transcriptomics) approaches^[79–84] also offer unique insight into biological processes involving melanins in various contexts.^[57] In the clinic it is useful to quickly and easily diagnose alkaptonuria using a

low-cost spectrophotometric technique for the detection of polyHGA;^[37] likewise, one of the potentially exciting applications of polyHGA is as a biocompatible intracellular label for optoacoustic imaging of macrophages with strong optoacoustic contrast to resolve single cells against a strong blood background.^[85]

3. Conclusion

Herein polymerization of HGA to form polyHGA (a simplified version of pyomelanin) was investigated in the absence or presence of enzymes (a laccase, peroxidase, or tyrosinase) at either pH 5.0 or 7.4. A variety of analytical techniques (UV–vis, NMR, XPS, SEC, DLS, SEM, EDX, FTIR, EPR, CV, and C-AFM) were employed to examine the polyHGAs produced under the experimental conditions. The experiments revealed interesting trends in the yields of polyHGAs produced with subtle differences in their properties; notably, C-AFM data for polyHGAs showed that those generated in the presence of LACC at pH 7.4, or HRP at pH 7.4 or 5.0, respectively, displayed measurable conductivity suggesting their potential for application in electronic devices.

4. Experimental Section

Materials: Unless otherwise noted, all chemicals and consumables were supplied by Sigma Aldrich (Merck), Gillingham, UK.

Polymerization of HGA (Lower Concentration of HGA—No Enzyme Control): HGA was dissolved in buffer (at a concentration of 0.052 g HGA in 5 mL of buffer solution, i.e., concentration of HGA of 10.4 mg mL^{−1}) at room temperature in the presence of air. The buffers were either sodium acetate (0.1 M, pH 5) or phosphate-buffered saline (0.1 M, pH 7.4) and if necessary, after the addition of HGA the pH was corrected by addition of 1 M NaOH or HCl. Samples were isolated at specific points in time before/after dialysis (molecular weight cutoff of 3.5 kDa) against water (4 L), refreshing the water every few hours for 5 days. The dialyzed mixtures were lyophilized (freeze dryer from Labconco Corporation), supplied by Thermo Fisher Scientific in Heysham, UK. Samples were stored in a freezer until analyzed.

Polymerization of HGA (Lower Concentration of HGA—in the Presence of Enzymes): HGA was dissolved in buffer (at a concentration of 0.052 g HGA in 5 mL of buffer solution, i.e., concentration of HGA of 10.4 mg mL^{−1}) at room temperature in the presence of air. The buffers were either sodium acetate (0.1 M, pH 5) or phosphate-buffered saline (0.1 M, pH 7.4) and, if necessary, after the addition of HGA the pH was corrected by addition of 1 M NaOH or HCl. Enzymatic polymerization reactions were initiated by addition of 85 units of enzyme chosen from HRP, supplied by Alfa Aesar (Thermo Fisher Scientific) in Heysham, UK, *Agaricus bisporus* LACC and mushroom TYR. Hydrogen peroxide (30%, 50 μ L) was added. Samples were isolated at specific points in time before/after dialysis (molecular weight cutoff of 3.5 kDa) against water (4 L), refreshing the water every few hours for 5 days. The dialyzed mixtures were lyophilized (freeze dryer from Labconco Corporation), supplied by Thermo Fisher Scientific in Heysham, UK. Samples were stored in a freezer until analyzed.

Polymerization of HGA (Higher Concentration of HGA—No Enzyme Control): HGA was dissolved in buffer (at a concentration of 0.168 g HGA in 5 mL of buffer solution, i.e., concentration of HGA of 33.6 mg mL^{−1}) at room temperature in the presence of air. The buffers were either sodium acetate (0.1 M, pH 5) or phosphate-buffered saline (0.1 M, pH 7.4) and, if necessary, after the addition of HGA the pH was corrected by addition

of 1 M NaOH or HCl. Samples were isolated at specific points in time before/after dialysis (molecular weight cutoff of 3.5 kDa) against water (4 L), refreshing the water every few hours for 5 days. The dialyzed mixtures were lyophilized (freeze dryer from Labconco Corporation), supplied by Thermo Fisher Scientific in Heysham, UK. Samples were stored in a freezer until analyzed.

Polymerization of HGA (Higher Concentration of HGA—in the Presence of Enzymes): HGA was dissolved in buffer (at a concentration of 0.168 g HGA in 5 mL of buffer solution, i.e., concentration of HGA of 33.6 mg mL^{−1}) at room temperature in the presence of air. The buffers were either sodium acetate (0.1 M, pH 5) or phosphate-buffered saline (0.1 M, pH 7.4) and, if necessary, after the addition of HGA the pH was corrected by addition of 1 M NaOH or HCl. Enzymatic polymerization reactions were initiated by addition of 170 units of enzyme chosen from HRP (supplied by Alfa Aesar (Thermo Fisher Scientific) in Heysham, UK), *Agaricus bisporus* LACC and mushroom TYR. Hydrogen peroxide (30%, 50 μ L) was added. Samples were isolated at specific points in time before/after dialysis (molecular weight cutoff of 3.5 kDa) against water (4 L), refreshing the water every few hours for 5 days. The dialyzed mixtures were lyophilized (freeze dryer from Labconco Corporation), supplied by Thermo Fisher Scientific in Heysham, UK. Samples were stored in a freezer until analyzed.

UV–Vis Spectroscopy: Spectra were recorded in UV Quartz cuvettes (Standard Cell with PTFE Stopper, manufactured in UV Quartz (195 nm to 2.5 μ m); path length = 10 mm, inside width = 10 mm, volume = 3.5 mL; outside dimensions (H \times W \times D) 45 \times 12.5 \times 12.5 mm.) on an Agilent Technologies Cary 60 UV–vis supplied by Thermo Fisher Scientific in Heysham, UK.

NMR Spectroscopy: ¹H NMR (400 MHz) spectra were recorded using a Bruker AVANCE III 400 NMR spectrometer using residual solvent as internal standards in deuterated solvents (D₂O). Chemical shift (δ) values were recorded in parts per million (ppm).

X-Ray Photoelectron Spectroscopy: A Kratos Analytical Axis Supra X-ray photoelectron spectrometer with a monochromatic Al K α source (1.487 keV) was used to analyze surface chemical composition.^[86,87] Powdered samples were mounted using carbon tape in a well-shaped holder. An internal flood gun was applied for neutralizing charging effects. Wide-scan and core-line spectra were recorded at pass energies of 160 and 20 eV and step sizes of 1 and 0.1 eV, respectively. Samples were measured in triplicate at an emission angle of 0° (relative to the surface normal), a power of 225 W (15 kV \times 15 mA), and an analysis area of 700 \times 300 μ m. Data were quantified and processed by CasaXPS (ver.2.3.23PR 1.0, Casa Software Ltd.) using linear baseline correction. All spectra were adjusted for charge compensation effects by offsetting the binding energy relative to the C–C component of the C 1s spectrum at 285.0 eV.

Size Exclusion Chromatography: Aqueous SEC was measured on a Jasco system equipped with a DG-2080-53 degasser, PU-980 pump, and an RI-2031 Plus refractive index detector (Jasco Deutschland Labor- und Dantentechnik GmbH, Groß-Umstadt, Germany) with 0.1 M Na₂HPO₄/0.05% NaN₃ pH 9 as an eluent and at a flow rate of 1 mL min^{−1} on a column set of PSS SUPREMA 1000 and 30 Å (10 μ m) at 30 °C (PSS, Mainz, Germany). Polyethyleneoxide (PEO) was used for calibration.^[50]

Dynamic Light Scattering: DLS measurements were performed using an ALV laser CGS3 Goniometer equipped with a 633 nm HeNe laser (ALV GmbH, Langen, Germany) at 25 °C and at a detection angle of 90°. The CONTIN analysis of the obtained correlation functions was performed using the ALV 7002 FAST Correlator Software.

Scanning Electron Microscopy: Prior to imaging, the samples were sputter-coated with a 10 nm layer of gold. The structures were observed using either a JEOL JSM–6390LV operating at 15 kV or a JEOL JSM 7800F scanning electron microscope (JEOL, Welwyn Garden City, UK) operating at 10–15 kV.

EDX Spectroscopy: For qualitative EDX analysis, the samples were sputter-coated with a layer of gold (60 s, 20 mA, 8 \times 10^{−2} mBar, \approx 5 nm) using a Quorum Q150RES sputter coater (Quorum Technologies Ltd.) and then investigated using a field-emission SEM JEOL JSM 7800F with an EDX system (X-Max50, Oxford Instruments, Abingdon, UK) at 10 mm working distance and 10 kV voltage mounted on a brass JEOL holder with 25 mm carbon tables (G3348N, Agar Scientific, Stansted, UK). Three

measurements were performed per sample and average results were presented.

FTIR Spectroscopy: All spectra were recorded using an Agilent Technologies Cary 630 FTIR instrument (Agilent Technologies Ltd., Cheshire, UK) at a resolution of 1 cm^{-1} and was an average of 16 scans.

EPR Spectroscopy: Room-temperature EPR spectra of polyHGA powders were recorded at X-band on a JEOL X320 spectrometer using 0.1 mW microwave power and 1 G modulation width (100 kHz modulation frequency). The g values were determined by using a Mn^{2+} marker. The spectra were simulated using EasySpin toolbox for MatLab.^[88]

Cyclic Voltammetry: Voltammetry was carried out using an EmStat 3+ potentiostat with PSTrace 4.7 software (PalmSens Houten, Netherlands) at ambient temperature. The cell was comprised of a three-electrode system with an Ag/AgCl reference electrode, a gold counter electrode, and a glassy carbon working electrode (GCE). The GCE was coated with a film prepared by drying 10 μL of a suspension of polyHGA (1 mg) in Nafion perfluorinated resin solution (10 μL of a 5 wt% in mixture of lower aliphatic alcohols and water, containing 45% water; product number 510211 from Sigma-Aldrich, Gillingham, UK) overnight in a fume hood at room temperature. Buffer (pH 5 or 7.4, described above) was used as the electrolyte, with a scan rate of 0.01 V s^{-1} between -1 and 1 V .

Conductive Probe AFM: A triangular bias voltage was applied on the AFM stage in electric contact with the samples. A Pt-coated AFM probe acted as a drain for the electric current. The electric signal collected by the conductive probe was fed into an I/V converter with a low-noise filter built in. Output current and bias voltage were recorded by an AFM controller in real time. Multiple $I-V$ traces were recorded and processed to extract the electrical conductance, which is an intrinsic property of the samples under investigation. The setup is depicted in Figure S35 (Supporting Information).

Supporting Information

Supporting Information is available from the Wiley Online Library or from the author.

Acknowledgements

The authors thank the Ministry of Education of Saudi Arabia and the Saudi Cultural Bureau for financial support for H.A.G. (Grant: KAU1526). J.G.H. thanks the UK Engineering and Physical Sciences Research Council for financial support (via Grant Nos. EP/R003823/1, EP/R511560/1, and EP/K03099X/1), and the UK Biotechnology and Biological Sciences Research Council for financial support (via Grant No. BB/L013797/1) and the UK Royal Society for financial support (via Grant No. RG160449). J.G.H. and R.L.M. thank the UK Medical Research Council (MRC) for financial support (via Grant No. MC_PC_17192). The authors thank Geoffrey R. Akien at Lancaster University for insightful discussions about NMR.

Conflict of Interest

The authors declare no conflict of interest.

Author Contributions

Conceptualization: J.G.H. and A.M.T.; methodology: all authors; formal analysis: all authors; investigation: H.A.G., A.L., A.R., K.K., J.E., S.J.B., M.D.A., and V.C.; writing—original draft preparation: H.A.G. and J.G.H.; writing—review and editing: all authors; supervision: B.J.R., F.H.S., A.M.T., and J.G.H.; project administration: A.M.T. and J.G.H.; funding acquisition: B.J.R., F.H.S., A.M.T., and J.G.H. All authors read and agreed to the published version of the manuscript.

Data Availability Statement

The data that support the findings of this study are available from the corresponding author upon reasonable request.

Keywords

alkaptonuria, conjugated polymers, melanins, organic electronics, pyromelanins

Received: December 14, 2021

Revised: January 13, 2022

Published online:

- [1] J. Zschocke, K. M. Gibson, G. Brown, E. Morava, V. Peters, *JIMD Reports*, Springer, Berlin **2015**. <https://doi.org/10.1007/978-3-662-48227-8>
- [2] G. Britton, *The Biochemistry of Natural Pigments*, Cambridge University Press, Cambridge **1983**.
- [3] F. Solano, *New J. Sci.* **2014**, 2014, 498276.
- [4] G. E. Costin, V. J. Hearing, *FASEB J.* **2007**, 21, 976.
- [5] P. A. Riley, *Int. J. Biochem. Cell Biol.* **1997**, 29, 1235.
- [6] B. Larsson, H. Tjälve, *Biochem. Pharmacol.* **1979**, 28, 1181.
- [7] J. M. Menter, *Polym. Int.* **2016**, 65, 1300.
- [8] M. d'Ischia, K. Wakamatsu, F. Cicoira, E. Di Mauro, J. C. Garcia-Borron, S. Commo, I. Galván, G. Ghanem, K. Kenzo, P. Meredith, A. Pezzella, C. Santato, T. Sarna, J. D. Simon, L. Zecca, F. A. Zucca, A. Napolitano, S. Ito, *Pigm. Cell Melanoma Res.* **2015**, 28, 520.
- [9] M. Xiao, M. D. Shawkey, A. Dhinojwala, *Adv. Opt. Mater.* **2020**, 8, 2000932.
- [10] A. D. Schweitzer, E. Revskaya, P. Chu, V. Pazo, M. Friedman, J. D. Nosanchuk, S. Cahill, S. Frases, A. Casadevall, E. Dadachova, *Int. J. Radiat. Oncol., Biol., Phys.* **2010**, 78, 1494.
- [11] S. Ito, K. Wakamatsu, *Pigm. Cell Res.* **2003**, 16, 523.
- [12] D. Sulzer, C. Cassidy, G. Horga, U. J. Kang, S. Fahn, L. Casella, G. Pezzoli, J. Langley, X. P. Hu, F. A. Zucca, I. U. Isaias, L. Zecca, *NPJ Parkinsons Dis.* **2018**, 4, 11.
- [13] R. Haining, C. Achat-Mendes, *Neural Regen. Res.* **2017**, 12, 372.
- [14] A. Mejía-Caballero, R. De Anda, G. Hernández-Chávez, S. Rogg, A. Martínez, F. Bolívar, V. M. Castaño, G. Gosset, *Microb. Cell Fact.* **2016**, 15, 161.
- [15] Q. Ye, F. Zhou, W. Liu, *Chem. Soc. Rev.* **2011**, 40, 4244.
- [16] M. Sugumaran, H. Barek, *Int. J. Mol. Sci.* **2016**, 17, 1753.
- [17] X. Chen, D. Xiao, X. Du, X. Guo, F. Zhang, N. Desneux, L. Zang, S. Wang, *Front. Physiol.* **2019**, 10, 1066.
- [18] M. J. Beltrán-García, F. M. Prado, M. S. Oliveira, D. Ortiz-Mendoza, A. C. Scalfo, A. Pessoa, M. H. G. Medeiros, J. F. White, P. Di Mascio, *PLoS One* **2014**, 9, e91616.
- [19] B. Roulier, B. Pérès, R. Haudecoeur, *J. Med. Chem.* **2020**, 63, 13428.
- [20] C. E. Turick, A. S. Knox, J. M. Becnel, A. A. Ekechukwu, C. E. Milliken, in *Biopolymers* (Ed: M. Elnashar), IntechOpen, London **2010**, Ch. 23.
- [21] L. Huang, M. Liu, H. Huang, Y. Wen, X. Zhang, Y. Wei, *Biomacromolecules* **2018**, 19, 1858.
- [22] A. A. R. Watt, J. P. Bothma, P. Meredith, *Soft Matter* **2009**, 5, 3754.
- [23] A. Büngeler, B. Hämis, O. Strube, *Int. J. Mol. Sci.* **2017**, 18, 1901.
- [24] R. L. Schroeder, K. L. Double, J. P. Gerber, *J. Chem. Neuroanat.* **2015**, 64–65, 20.
- [25] V. B. Yerger, R. E. Malone, *Nicotine Tob. Res.* **2006**, 8, 487.
- [26] F. Solano, *Int. J. Mol. Sci.* **2017**, 18, 1561.
- [27] H. A. Galeb, E. L. Wilkinson, A. F. Stowell, H. Lin, S. T. Murphy, P. L. Martin-Hirsch, R. L. Mort, A. M. Taylor, J. G. Hardy, *Global Challenges* **2021**, 5, 2000102.

- [28] W. Cao, X. Zhou, N. C. McCallum, Z. Hu, Q. Z. Ni, U. Kapoor, C. M. Heil, K. S. Cay, T. Zand, A. J. Mantanona, A. Jayaraman, A. Dhinojwala, D. D. Deheyn, M. D. Shawkey, M. D. Burkart, J. D. Rinehart, N. C. Gianneschi, *J. Am. Chem. Soc.* **2021**, *143*, 2622.
- [29] R. L. Mort, I. J. Jackson, E. E. Patton, *Development* **2015**, *142*, 620.
- [30] M. D'ischia, A. Napolitano, A. Pezzella, P. Meredith, M. Buehler, *Angew. Chem., Int. Ed.* **2020**, *59*, 11196.
- [31] M. Al Khatib, J. Costa, D. Spinelli, E. Capecci, R. Saladino, M. C. Baratto, R. Pogni, *Int. J. Mol. Sci.* **2021**, *22*, 1739.
- [32] A. M. Taylor, K. P. Vercruysse, in *JIMD Reports* (Eds: E. Morava, M. Baumgartner, M. Patterson, S. Rahman, J. Zschocke, V. Peters), Vol. 35, Springer, Berlin **2017**, pp. 79–85.
- [33] W. Y. Chow, A. M. Taylor, D. G. Reid, J. A. Gallagher, M. J. Duer, *J. Inherited Metab. Dis.* **2011**, *34*, 1137.
- [34] L. Ranganath, A. M. Taylor, A. Shenkin, W. D. Fraser, J. Jarvis, J. A. Gallagher, N. Sireau, *J. Inherited Metab. Dis.* **2011**, *34*, 723.
- [35] A. M. Taylor, B. Wlodarski, I. A. Prior, P. J. M. Wilson, J. C. Jarvis, L. R. Ranganath, J. A. Gallagher, *Rheumatology* **2010**, *49*, 1412.
- [36] F. Lorquin, F. Ziarelli, A. Amouric, C. Di Giorgio, M. Robin, P. Piccerelle, J. Lorquin, *Sci. Rep.* **2021**, *11*, 8538.
- [37] Y. Tokuhara, K. Shukuya, M. Tanaka, K. Sogabe, Y. Ejima, S. Hosokawa, H. Ohsaki, T. Morinishi, E. Hirakawa, Y. Yatomi, T. Shimomura, *Sci. Rep.* **2018**, *8*, 11364.
- [38] S. Castro-Sowinski, G. Martinez-Drets, Y. Okon, *FEMS Microbiol. Lett.* **2002**, *209*, 119.
- [39] G. Bayramoğlu, M. Y. Arica, *J. Hazard. Mater.* **2008**, *156*, 148.
- [40] M. Masuda, A. Sakurai, M. Sakakibara, *World J. Microbiol. Biotechnol.* **2002**, *18*, 739.
- [41] K. Ikehata, *Bioresour. Technol.* **2000**, *74*, 191.
- [42] M. D'ischia, A. Napolitano, G. Prota, *Biochim. Biophys. Acta, Gen. Subj.* **1991**, *1073*, 423.
- [43] S. Kobayashi, H. Higashimura, *Prog. Polym. Sci.* **2003**, *28*, 1015.
- [44] J. López, J. M. Hernández-Alcántara, P. Roquero, C. Montiel, K. Shirai, M. Gimeno, E. Bárcana, *J. Mol. Catal. B: Enzym.* **2013**, *97*, 100.
- [45] M. Ghoul, L. Chebil, in *Enzymatic Polymerization of Phenolic Compounds by Oxidoreductases*, Springer, Dordrecht **2012**, pp. 1–46. <https://doi.org/10.1007/978-94-007-3919-2>
- [46] M. L. Sánchez-Mundo, V. M. Escobedo-Crisantes, S. Mendoza-Arvizu, M. E. Jaramillo-Flores, *CyTA - J. Food* **2016**, *14*, 594.
- [47] H. Tonami Ph.D., Kyoto University 2003.
- [48] A. C. Ferrari, F. Bonaccorso, V. Fal'ko, K. S. Novoselov, S. Roche, P. Boggild, S. Borini, F. H. L. Koppens, V. Palermo, N. Pugno, J. A. Garrido, R. Sordan, A. Bianco, L. Ballerini, M. Prato, E. Lidorikis, J. Kivioja, C. Marinelli, T. Ryhänen, A. Morpurgo, J. N. Coleman, V. Nicolosi, L. Colombo, A. Fert, M. Garcia-Hernandez, A. Bachtold, G. F. Schneider, F. Guinea, C. Dekker, M. Barbone, et al., *Nanoscale* **2015**, *7*, 4598.
- [49] Y. Topal, S. Tapan, E. Gokturk, E. Sahmetlioglu, *J. Saudi Chem. Soc.* **2017**, *21*, 731.
- [50] J. B. Max, P. J. Mons, J. C. Tom, F. H. Schacher, *Macromol. Chem. Phys.* **2020**, *221*, 1900383.
- [51] J. C. F. Alves, J. A. Freire, *Macromol. Theory Simul.* **2018**, *27*, 1800020.
- [52] I. A. Menon, S. D. Persad, H. F. Haberman, P. K. Basu, J. F. Norfray, C. C. Felix, B. Kalyanaraman, *Biochem. Cell Biol.* **1991**, *69*, 269.
- [53] A. B. Mostert, G. R. Hanson, T. Sarna, I. R. Gentle, B. J. Powell, P. Meredith, *J. Phys. Chem. B* **2013**, *117*, 4965.
- [54] M. Eslami, H. R. Zare, M. Namazian, *J. Electroanal. Chem.* **2014**, *720*–721, 76.
- [55] M. Eslami, M. Namazian, H. R. Zare, *J. Phys. Chem. B* **2013**, *117*, 2757.
- [56] S. Dubey, D. Singh, R. A. Misra, *Enzyme Microb. Technol.* **1998**, *23*, 432.
- [57] P. Meredith, T. Sarna, *Pigm. Cell Res.* **2006**, *19*, 572.
- [58] M. A. Dubé, S. Salehpour, *Macromol. React. Eng.* **2014**, *8*, 7.
- [59] T. Eom, K. Woo, W. Cho, J. E. Heo, D. Jang, J. I. Shin, D. C. Martin, J. J. Wie, B. S. Shim, *Biomacromolecules* **2017**, *18*, 1908.
- [60] L. Migliaccio, P. Manini, D. Altamura, C. Giannini, P. Tassini, M. G. Maglione, C. Minarini, A. Pezzella, *Frontiers in Chemistry* **2019**, *7*, 162.
- [61] J. V. Paulin, A. P. Coleone, A. Batagin-Neto, G. Burwell, P. Meredith, C. F. Graeff, A. B. Mostert, *J. Mater. Chem. C* **2021**, *9*, 8345.
- [62] M. I. N. Da Silva, S. N. Dezidério, J. C. Gonzalez, C. F. O. Graeff, M. A. Cotta, *J. Appl. Phys.* **2004**, *96*, 5803.
- [63] J. P. Bothma, J. De Boer, U. Divakar, P. E. Schwen, P. Meredith, *Adv. Mater.* **2008**, *20*, 3539.
- [64] E. Vahidzadeh, A. P. Kalra, K. Shankar, *Biosens. Bioelectron.* **2018**, *122*, 127.
- [65] P. Zheng, B. Ding, G. Li, *Macromol. Biosci.* **2020**, *20*, 2000228.
- [66] S. Wang, Q. Liu, L. Li, M. W. Urban, *Macromol. Rapid Commun.* **2021**, *42*, 2100054.
- [67] D. Cui, C. Xie, K. Pu, *Macromol. Rapid Commun.* **2017**, *38*, 1700125.
- [68] J. H. Ryu, P. B. Messersmith, H. Lee, *ACS Appl. Mater. Interfaces* **2018**, *10*, 7523.
- [69] D. Amin, C. Sugnaux, K. Lau, P. Messersmith, *Biomimetics* **2017**, *2*, 17.
- [70] A. Banerjee, S. Ray, *Gene* **2016**, *592*, 99.
- [71] C. Olivares, F. Solano, *Pigm. Cell Melanoma Res.* **2009**, *22*, 750.
- [72] S. V. S. Kumar, P. S. Phale, S. Durani, P. P. Wangikar, *Biotechnol. Bioeng.* **2003**, *83*, 386.
- [73] Y.-T. Chien, S.-W. Huang, *PLoS One* **2012**, *7*, e47951.
- [74] A. J. M. Ribeiro, J. D. Tyzack, N. Borkakoti, G. L. Holliday, J. M. Thornton, *J. Biol. Chem.* **2020**, *295*, 314.
- [75] T. Zhang, H. Zhang, K. Chen, S. Shen, J. Ruan, L. Kurgan, *Bioinformatics* **2008**, *24*, 2329.
- [76] K. Choi, S. Kim, *J. Bioinf. Comput. Biol.* **2011**, *9*, 597.
- [77] I. Shah, L. Hunter, *Proc. Int. Conf. Intell. Syst. Mol. Biol.* **1997**, *5*, 276.
- [78] M. Gauden, A. Pezzella, L. Panzella, M. T. Neves-Petersen, E. Skovsen, S. B. Petersen, K. M. Mullen, A. Napolitano, M. D'ischia, V. Sundström, *J. Am. Chem. Soc.* **2008**, *130*, 17038.
- [79] M. A. Durante, D. A. Rodriguez, S. Kurtenbach, J. N. Kuznetsov, M. I. Sanchez, C. L. Decatur, H. Snyder, L. G. Feun, A. S. Livingstone, J. W. Harbour, *Nat. Commun.* **2020**, *11*, 496.
- [80] R. L. Belote, D. Le, A. Maynard, U. E. Lang, A. Sinclair, V. Planells-Palop, L. Baskin, A. D. Tward, S. Darmanis, R. L. Judson-Torres, *Nat. Cell Biol.* **2021**, *23*, 1035.
- [81] Z. Abattayani, L. Xerri, J. Hassoun, J.-J. Bonerandi, J.-J. Grob, *Pigm. Cell Res.* **1993**, *6*, 400.
- [82] T. H. P. Atlas Lacc, <https://www.proteinatlas.org/ENSG00000179630-LACC1/tissue> (accessed: August 2021).
- [83] T. H. P. Atlas TYR, <https://www.proteinatlas.org/ENSG00000077498-TYR/tissue> (accessed: August 2021).
- [84] E. Atlas, Gene expression across species and biological conditions, <https://www.ebi.ac.uk/gxa/experiments/E-MTAB-3358/Results> (accessed: August 2021).
- [85] I. Weidenfeld, C. Zakian, P. Duewell, A. Chmyrov, U. Klemm, J. Aguirre, V. Ntziachristos, A. C. Stiel, *Nat. Commun.* **2019**, *10*, 5056.
- [86] G. Beamson, D. Briggs, *High Resolution XPS of Organic Polymers: The Scienta ESCA300 Database*, John Wiley & Sons, Chichester **1992**. <https://analyticalsciencejournals.onlinelibrary.wiley.com/doi/pdf/10.1002/sia.740200310>
- [87] J. F. Moulder, W. F. Stickle, P. E. Sobol, K. D. Bomben, *Handbook of X-Ray Photoelectron Spectroscopy* (Eds: J. Chastain, R. C. King Jr.), Perkin-Elmer, Eden Prairie, MN **1992**, p. 261.
- [88] Easy spin. <https://easyspin.org/> (accessed: January 2022).